International Journal of Research in Civil Engineering and Technology

E-ISSN: 2707-8272
P-ISSN: 2707-8264
Impact Factor (RJIF): 5.44
IJRCET 2026; 7(1): 69-81
[Journal's Website](#)
Received: 04-11-2025
Accepted: 06-12-2025

Andini Triherdi Utami
Student, Department of Civil Engineering, Universitas Negeri Semarang, Semarang, Indonesia

Arief Kusbiantoro
Department of Civil Engineering, Universitas Negeri Semarang, Semarang, Indonesia

Rini Kusumawardani
Department of Civil Engineering, Universitas Negeri Semarang, Semarang, Indonesia

Indah Maharani
Student, Department of Civil Engineering, Universitas Negeri Semarang, Semarang, Indonesia

Hadi Yudariansyah
Professional Engineer Program, Faculty of Engineering, Universitas Diponegoro, Semarang, Indonesia

Rohana Hassan
1. Faculty of Civil Engineering, Universiti Teknologi MARA (UiTM), Shah Alam, Selangor, Malaysia
2. Institute for Infrastructure Engineering and Sustainable Management (IIESM), Universiti Teknologi MARA, 40450 Shah Alam, Selangor Darul Ehsan, Malaysia

Corresponding Author:
Arief Kusbiantoro
Department of Civil Engineering, Universitas Negeri Semarang, Semarang, Indonesia

Assessment of the behavior of railway bridge piers under seismic load using pushover analysis

Andini Triherdi Utami, Arief Kusbiantoro, Rini Kusumawardani, Indah Maharani, Hadi Yudariansyah and Rohana Hassan

DOI: https://www.doi.org/10.22271/27078264.2026.v7.i1b.119

Abstract
The construction of railroad bridges aims to redirect traffic and mitigate congestion in high-density areas. This study involves 3D finite element modeling of a double-track steel frame bridge using CSi Bridge software based on engineering design data. Seismic analysis results for the six pillars show maximum displacements of 35.3208 mm in the longitudinal direction (X-axis) and 29.7877 mm in the transverse direction (Y-axis). The structural integrity is confirmed by a demand-to-capacity ratio of 0.268, significantly below the safety threshold of 1.0. Load analysis indicates that the long-span condition with two passing trains generates the highest stress, reaching a maximum moment of 2.00 x 10^4 kNm and a shear force of 8.64 x 10^3 kN. These values exceed those recorded for single-train or short-span scenarios. Overall, the analysis demonstrates that the bridge design is structurally sound and safely accommodates both seismic forces and operational train loads.

Keywords: Pushover analysis, displacement, moment value, shear force, Railways Bridge

1. Introduction

Nuranita (2023) [13] defined railroad bridges as infrastructure built to move railroad traffic over obstacles. According to national transportation development data released by the Central Bureau of Statistics (2023), the number of train passengers reached 270 million cumulatively during the period from January to September 2023, representing a 40.06% increase compared to the same period in 2022. Regulation of the Minister of Transportation No. 60 of 2012 defines a train as a means of public transportation with motive power, either running alone or coupled with other vehicles, that moves along rail lines associated with train travel.

Guo *et al.* (2019) [5] found that the pillar, which is one of the important components of the railway bridge structure, is designed based on its stiffness. The pillar has a large cross-section, allowing it to meet the traffic safety requirements of the railway bridge. Krawinkler *et al.* (1998) [6] and Bagch *et al.* (2023) [2] studied the structural planning of bridge pillars, which involves identifying structural capacity parameters, determining acceptable values, and predicting the demand caused by seismic forces. Vičan *et al.* (2016) [18] and Bencardino (2023) found the failure and damage include imperfections of structural components that must be implemented into the bridge computational model appropriately to allow for their influence on the final response of the bridge to all loads because the performance deficit may be due to progressive damage from external actions, natural deterioration including material decay, structural inadequacy, events such as earthquakes, but also increased loads and vehicle speeds to which bridges originally designed for wagon passage are subjected. Bridges damaged by large earthquakes due to inadequate pillar planning can have a profoundly hazardous impact on society, as they obstruct transportation and emergency rescue efforts. The repair of buildings after earthquakes is difficult and costly, as studied by Chen *et al.* (2023) [3], Zhang *et al.* (2020) [22], and Mosleh et al. (2016) [12]. The substantial horizontal load caused the shear capacity of the central column to reach its yield point, gradually producing damage. Then, the vertical bearing capacity of the column slowly decreased, and overall compression-bending damage occurred under the continuing loadings. Yamato *et al.* (1996) [20] found the strain generated in the central columns was five times higher than that in the side walls. The central columns were damaged due to insufficient shear bearing capacity, which led to the collapse of the top slab, as studied by Yang *et al.* (2023) [21].

Pushover analysis is a widely used research method to evaluate seismic forces on bridge structures. The pushover analysis approach requires the identification of research review modal parameters to extract characteristics of the bridge structural system, suitable for subsequent updating of the finite element model (FEM), as studied by Wu *et al*. (2022) [19]. A proper finite element model can usually be developed by first drawing and then followed by accurate calibration using reliable modal parameters, as seen in recent studies by Kusumawardani *et al*. (2023) [11]. The finite element model was built based on the identified frequency and shape vectors by adjusting the girder and pier connections with rotational springs to reflect the actual conditions, and the accuracy was shown to be less than 1% error for the first two vertical bending modes, as studied by Wu *et al*. (2022) [19]. Kusbiantoro *et al*. (2023) [11] conducted a seismic performance analysis for a double-track railway bridge subjected to moderate to strong earthquake accelerations in both longitudinal and transverse directions. Kusumawardani *et al*. (2024) [9] found that damage to the structure results in a permanent change in the stiffness distribution of the structure, and these changes can be detected through monitoring the vibrations that occur within the structure.

Capacity is the ability of a structure to resist seismic demand. The value of structural capacity depends on the strength and deformation ability of each component of the structure. The demand, in the form of elastic spectrum response with 5% damping, is studied by Riyono *et al*. (2023) [14] as an earthquake load.

Shatarat *et al*. (2017) [16] found that pushover Analysis is not a recent advancement; it has been developed since the 1970s. Validity testing and related applications of pushover analysis in seismic assessment of buildings and bridges have been extensively researched. Bridges are structures with a more important or critical role than buildings; developing pushover analysis procedures for bridge structures is a challenge. Some of the functions of applying pushover analysis to bridges include calculating seismic forces in nonlinear systems, which consist of two stages: the highest response inelastic degree of freedom and the total demand, by combining modal combinations as studied by Chopra *et al*. (2001) [4].

Kusumawardani *et al*. (2019) [8] compared the size vibrations caused by the train, which can be seen from the mark acceleration, amplitude, and frequency. The vibration Frequency experience is frequency dominant in a system when experiencing vibration without existing damping. Suhary (2000) [17] found that when the wheel train passes over the iron rails and sleepers, it results in a large frequency-influenced speed moment of the train. A load test is beneficial for measuring the frequency of bridge experiences, as studied by Setiati *et al*. (2013) [15]. A carload of flames passing at a certain speed can produce transmitted vibrations through the wheel train, which are then transferred to the steel rail, causing a fire, and subsequently to the ballast, and distributed to the land base. The size vibrations caused by the train fire can be seen from the mark acceleration, amplitude, and frequency of the vibration. Kusbiantoro *et al*. (2025) [10] studied modal analysis is essential for accurately identifying the dynamic properties of a bridge, which are required to evaluate its real structural behavior and to develop a reliable finite element model for further assessment.

2. Methods

2.1 Bridge Description

The steel truss railway double-track bridge is located in Central Java Province, Indonesia, as shown in Figure 1. Most of the elements of the bridge are a pipe truss. The bridge truss is divided into three parts: the lower truss, which serves as the main girder, the upper truss, and the bracing truss. The steel frame bridge has a length of 270 m, with three main spans, as shown in Figure 3. The steel truss railroad double-track bridge features six reinforced concrete main piers, as illustrated in Figure 4. Figure 2 presents a detailed schematic view of a bridge cross-section. The total width of this double-track bridge is 14.1 m. Side barriers or parapets flank the deck, providing multiple lanes to accommodate two-way train traffic. Below the deck, a series of supporting elements, including beams, girders, and trusses, offers vertical and horizontal load-bearing capacity. These elements are arranged symmetrically, ensuring that the loads from the bridge deck are distributed evenly to the underlying support structure.

Fig 1: Research location

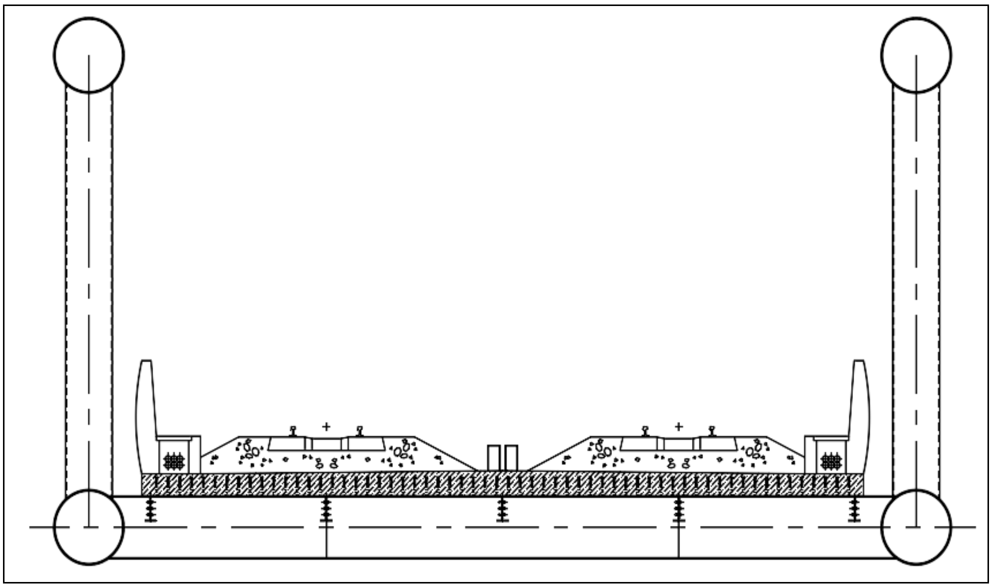

Fig 2: Cross section

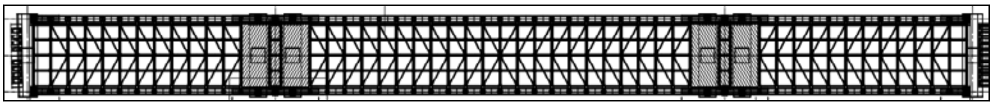

Fig 3: Top view

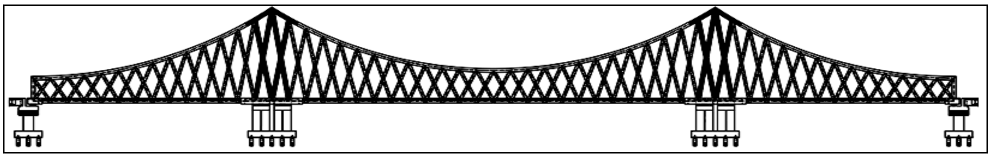

Fig 4: Side view

2.2 3D Finite Element Bridge Model

Figure 5 presents a 3D representation model of a bridge structure using the finite element model. The model provides a clear visualization of the interaction between the bridge's supports and the deck, capturing the geometric arrangement of the structure for analysis. The global coordinate system is illustrated, featuring the X, Y, and Z axes. This indicates the orientation of the model for analysis, where the X-axis represents the longitudinal direction along the bridge span, the Y-axis represents the lateral direction, perpendicular to the bridge's length, and the Z-axis represents the vertical direction, perpendicular to the ground. This finite element model is crucial for simulating the bridge's response to different loads and conducting structural analysis to evaluate its performance, strength, and safety under various scenarios. The spans are identified with their respective lengths: two side spans of 70 meters each and a longer central span of 130 meters. The bridge structure is a complex truss system, with triangular configurations forming the primary structural elements of the bridge deck and supporting framework.

The trusses span the entire length of the bridge, ensuring even load distribution and overall structural integrity. The main girder used on the bridge uses a steel pipe with a diameter of 1200 mm and a thickness of 22 mm. The bridge cross girder uses 900×600×24×24 steel hollow profiles, which were installed at 5 m intervals along the bridge's length, with a total length of 14100 mm. The bridge stringers, which use WF 400×200×8×13 profiles, are installed lengthwise in the direction of the bridge, every 3 m from the bridge axle, and have a length of 5 m. The steel frame railroad double-track bridge is a type of bridge with a pipe truss. The lower truss has a diameter of 1200 mm and a thickness of 22 mm; the upper truss has a diameter of 1200 mm and a thickness of 22 mm, while the bracing truss has a diameter of 800 mm and a thickness of 14 mm. The bridge consists of multiple spans supported by piers (PIER 1 through PIER 6) strategically located along the length of the structure. The six piers provide vertical support for the bridge at key intervals, ensuring stability and load transfer to the foundations. Each pier is modeled with specific boundary conditions and structural properties that influence how the bridge behaves under various loads, such as seismic forces or train-induced dynamic loads. The pier of this bridge is constructed directly from reinforced concrete with a concrete quality of f'c 30 MPa and reinforcement steel diameters of 19 & 25 mm. The pier height is 6750 mm. The pierhead of this bridge uses directly cast reinforced concrete with a concrete quality f'c 41.5 Mpa and a reinforcement steel diameter of 25.

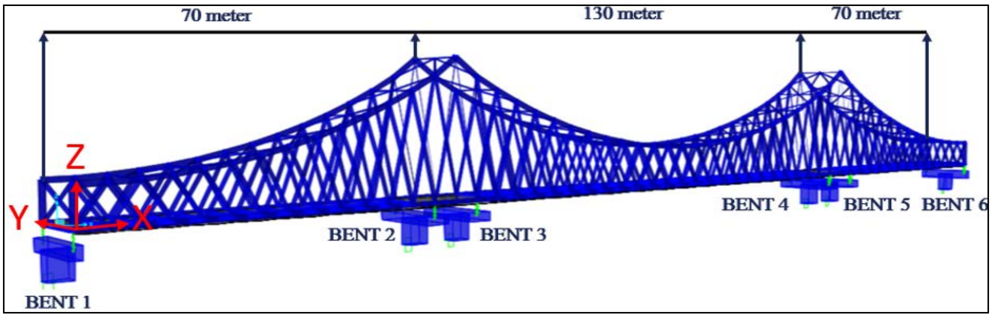

Fig 5: Finite element model

3. Result

3.1 Result of Pushover Analysis of 3D FEM

Figure 6 presents a pushover curve for Pier 1 in the transverse and longitudinal direction; the blue line illustrates the relationship between base shear and displacement. The curve initially displays a linear increase in base shear with increasing displacement, reaching a maximum base shear value of approximately 1100 kN at around 30 mm displacement. Beyond this point, the curve exhibits a plateau, indicating that further displacement does not significantly increase base shear. This behavior suggests that the structure reaches its capacity to resist additional forces, marking the onset of a stable plastic deformation phase. The graph effectively captures the structural performance under lateral load conditions, highlighting the elastic and plastic response phases. The orange line illustrates the pushover curve for Pier 1 in the longitudinal direction, depicting the relationship between base shear and displacement. The base shear reaches a peak value of approximately 1400 kN at around 35 mm displacement. Beyond this point, the curve flattens, signifying that the structure has reached its ultimate capacity and is undergoing plastic deformation. The plateau in the curve represents the transition from elastic to plastic behavior, where further displacement does not lead to an increase in base shear.

Figure 7 illustrates the pushover curve for Pier 2 in both the transverse and longitudinal directions; the blue line represents the relationship between base shear and displacement. The maximum base shear reaches approximately 1400 kN at around 35 mm of displacement. After this peak, the curve flattens, indicating that the structure has reached its capacity and has entered the plastic deformation phase. Further increases in displacement do not result in additional base shear, signifying that the structure has exhausted its load-carrying capacity in the transverse direction. The orange line presents the pushover curve for Pier 2 in the longitudinal direction, showing the relationship between base shear and displacement. The base shear reaches a maximum value of approximately 2000 kN at around 12 mm of displacement. Beyond this point, the curve flattens, signifying that the structure has reached its ultimate load-bearing capacity, and further displacement results in no significant increase in base shear. This plateau indicates the onset of plastic deformation, where the structure undergoes permanent deformation without gaining additional strength.

Figure 8 illustrates the pushover curve for Pier 3 in the transverse and longitudinal direction; the blue represents the relationship between base shear and displacement. The base shear reaches a maximum value of approximately 1700 kN at around 35 mm of displacement. After this peak, the curve enters a plateau phase, indicating that the structure has reached its maximum load-carrying capacity and is now experiencing plastic deformation. In this phase, additional displacement does not increase base shear. This behavior signifies the transition from elastic to plastic deformation, providing insight into the structure's capacity to withstand transverse loads before experiencing permanent damage. The orange presents the pushover curve for Pier 3 in the longitudinal direction, showing the relationship between base shear and displacement. The base shear reaches its maximum value of approximately 1800 kN at around 13 mm displacement. Beyond this point, the curve flattens, indicating the onset of plastic deformation, where the structure has reached its load-carrying capacity and further displacement does not increase base shear. This behavior highlights the structure's performance under longitudinal loading, indicating both its elastic and plastic phases, and marking the point at which permanent deformations occur.

Figure 9 depicts the pushover curve for Pier 4 in the transverse and longitudinal direction. The x-axis represents the lateral displacement in millimeters (mm), while the y-axis indicates the corresponding base shear in kilonewtons (kN). The base shear initially increases linearly with displacement, indicating elastic behavior. The curve with blue line reaches a peak base shear of approximately 1450 kN at 27 mm displacement. After this point, the curve also plateaus, signifying the structure's transition from elastic to inelastic behavior and its capacity to sustain further displacements without a corresponding increase in base shear.

The orange line illustrates the pushover curve in the longitudinal direction. The curve exhibits an initial linear increase in base shear with displacement, reaching a peak of approximately 2200 kN at 12 mm displacement. Beyond this point, the curve plateaus, indicating that the structural system has reached its yield capacity and enters a plastic behavior phase with no significant increase in base shear despite further displacement. This plateau suggests the onset of nonlinear behavior and energy dissipation through plastic hinge formation or other inelastic mechanisms. The structure exhibits higher lateral strength but lower ductility in the longitudinal direction, whereas in the transverse direction, it has greater ductility but lower strength.

Figure 10 presents the pushover curves for Pier 5 in both transverse and longitudinal directions, illustrating the structural response under lateral loading conditions.

The blue line depicts the pushover curve of Pier 5 in the transverse direction. The x-axis represents the lateral displacement in millimeters (mm), while the y-axis indicates the base shear in kilonewtons (kN). The curve demonstrates an initial linear increase in base shear with displacement, signifying elastic behavior up to approximately 28 mm of displacement, where the base shear reaches a peak of approximately 1500 kN. Beyond this point, the curve exhibits a plateau, indicating that the structure has entered the plastic range and is undergoing inelastic deformations without a significant increase in base shear capacity.

The orange shows the pushover curve of Bent 5 in the longitudinal direction. Similar to Figure 14, the base shear increases linearly with displacement, indicating elastic behavior until around 14 mm of displacement, at which point the base shear reaches approximately 1800 kN. A plateau follows this point, suggesting the onset of plastic behavior. Compared to the transverse direction, the longitudinal response displays a higher peak base shear and a steeper initial slope, indicating greater stiffness and strength along the longitudinal axis.

Figure 11 shows the pushover curve of Bent 6 in the transverse and longitudinal directions. The blue curve exhibits a typical bilinear behavior. Initially, the structure responds elastically, with base shear increasing linearly with displacement up to approximately 28 mm, reaching a base shear capacity of around 1100 kN. Beyond this point, the curve plateaus, indicating that the structure has yielded and entered a plastic stage where further displacement does not result in significant increases in base shear. This suggests that the transverse capacity of the structure is governed by ductile mechanisms post-yielding.

The orange curve presents the pushover curve of Bent 6 in the longitudinal direction. Similar to the transverse case, the curve also displays bilinear characteristics. The structure remains in the elastic range until approximately 30 mm of displacement, at which point it reaches a peak base shear of approximately 1400 kN. Thereafter, the curve levels off, indicating a transition into the plastic phase. Compared to the transverse direction, the longitudinal direction exhibits a higher base shear capacity, indicating greater stiffness and strength along this axis.

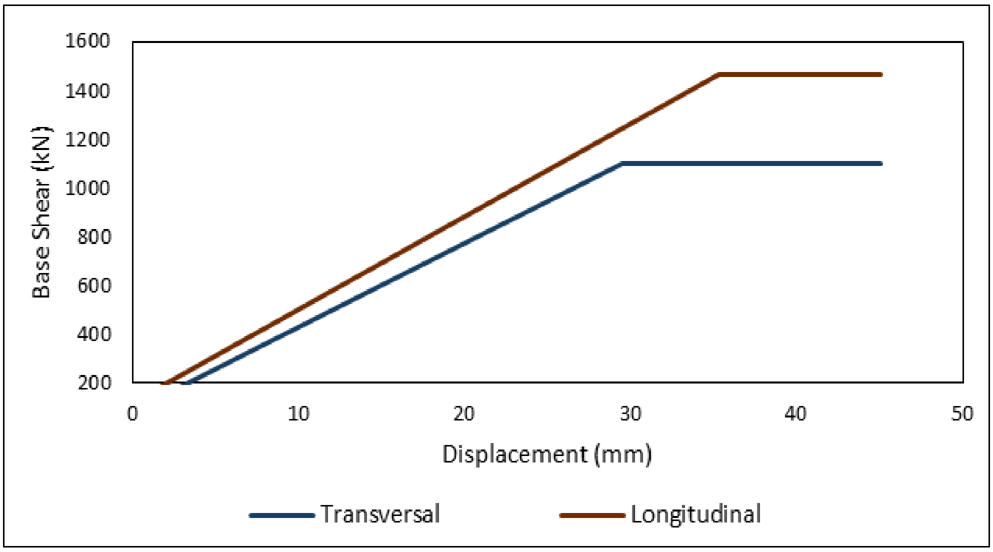

Fig 6: Pushover curve pier 1

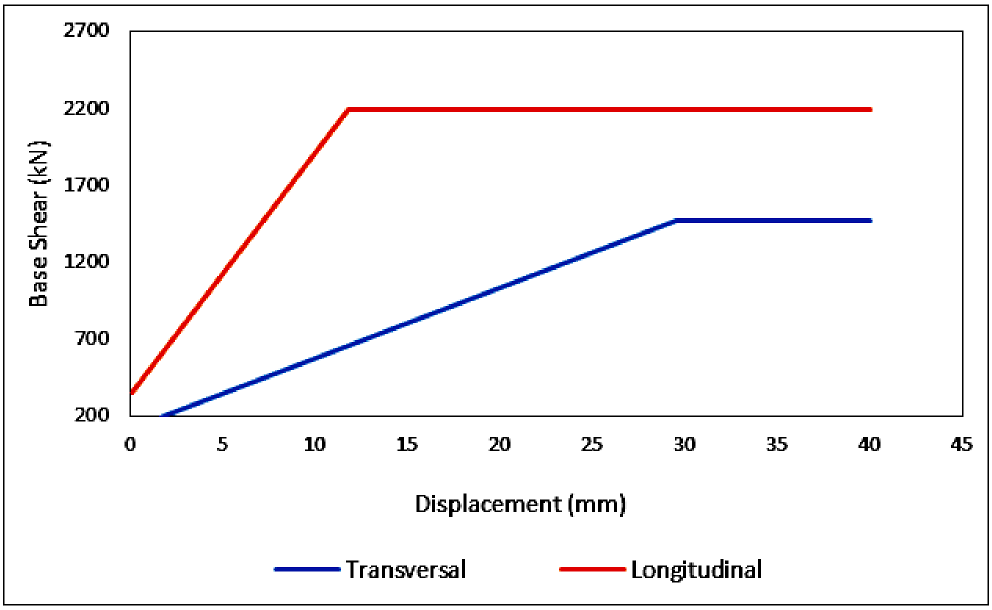

Fig 7: Pushover curve pier 2

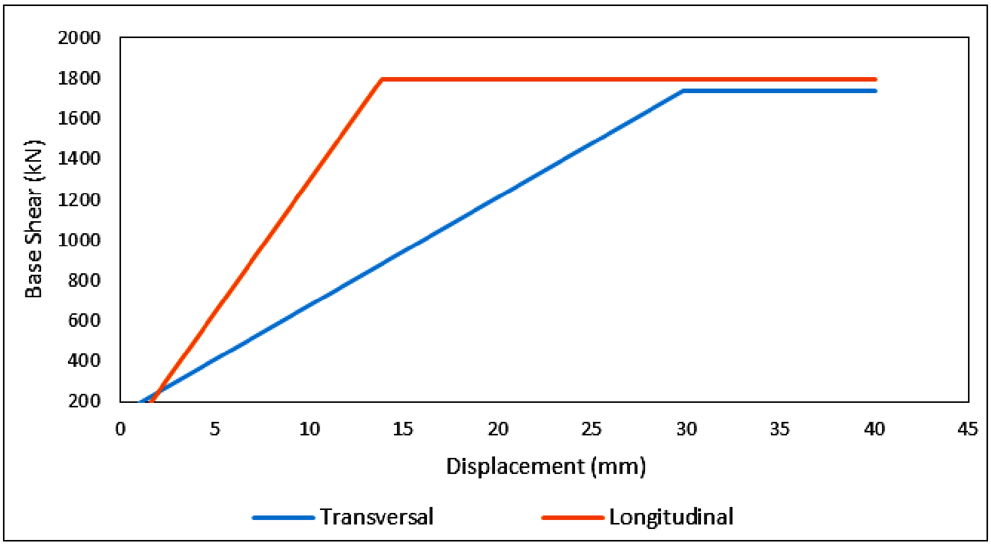

Fig 8: Pushover curve pier 3

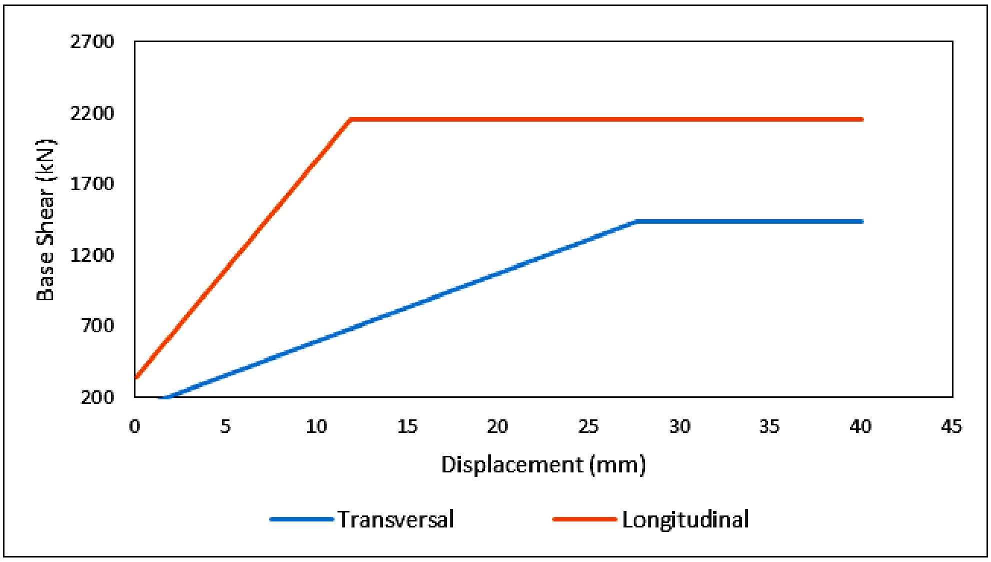

Fig 9: Pushover curve pier 4

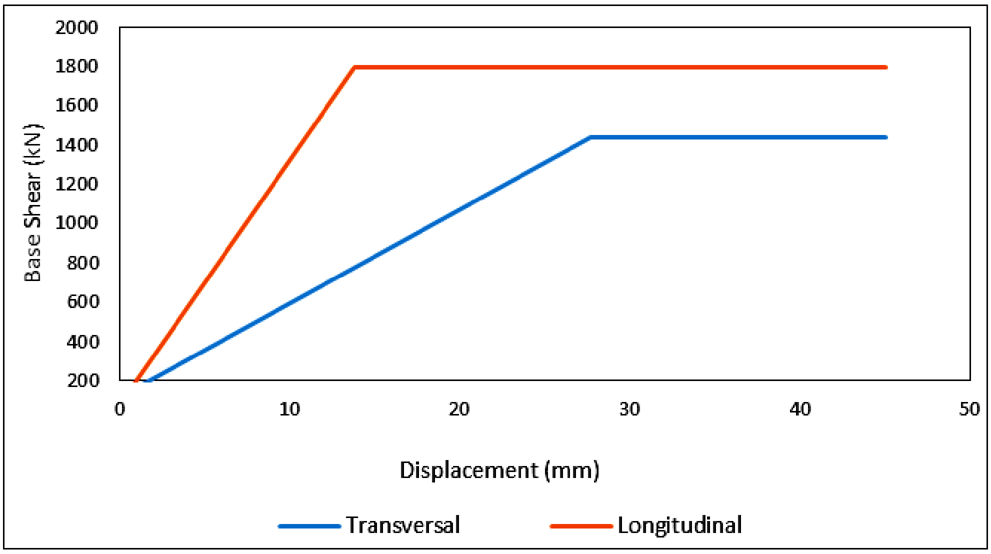

Fig 10: Pushover curve pier 5

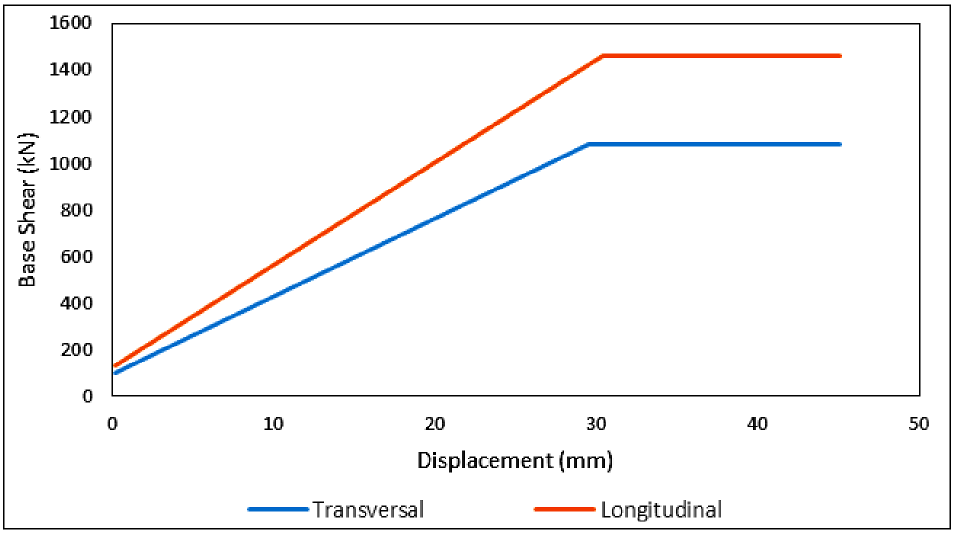

Fig 11: Pushover curve pier 6

This is a recapitulation of the base shear and displacement values obtained from the Csi Bridge software analysis in Table 1 below.

Table 1: scenario Recapitulation of base shear and displacement values

	Base Shear (kN)		**Displacement (mm)**	
	Transverse (Y-axis)	**Longitudinal (X-axis)**	**Transverse (Y-axis)**	**Longitudinal (X-axis)**
1	1095.97	1461.30	29.43	35.32
2	1461.30	2191.95	29.43	11.77
3	1733.75	1795.67	29.79	13.82
4	1436.53	2154.80	27.64	11.82
5	1436.53	1795.67	27.64	13.82
6	1077.40	1461.30	29.43	30.32

For the result of base shear, the base shear values represent the lateral forces resisted by the pier due to seismic loads. These values are reported in both the transverse (Y-axis) and longitudinal (X-axis) directions. Pier 1 experiences a base shear of 1095.97 kN in the transverse direction and 1461.30 kN in the longitudinal direction. Pier 2 shows higher base shear values, with 1461.30 kN in the transverse direction and 2191.95 kN in the longitudinal direction. The largest base shear values are observed at Pier 3, with 1733.75 kN in the transverse direction and 1795.67 kN in the longitudinal direction, indicating that this Pier resists the highest lateral forces. For displacement, the displacement values represent the movement or deformation of the piers due to seismic loads, reported for both the transverse and longitudinal directions. In the transverse direction, the displacement values range from 29.43 mm (Pier 1) to 29.79 mm (Pier 3), indicating minimal variation in transverse movement across the piers. In the longitudinal direction, Pier 1 shows the highest displacement of 35.32 mm. The table provides a comprehensive overview of the structural response of the bridge's piers under seismic loading. Pier 3 experiences the highest base shear in both directions, reflecting its critical role in resisting seismic forces. In contrast, Pier 1 and Pier 3 exhibit the largest displacements, particularly in the longitudinal direction. The data suggest that different piers play varying roles in resisting shear forces and accommodating displacement, emphasizing the importance of understanding the specific demands on each Pier during seismic events. Based on the results of the seismic analysis of the bridge using pushover analysis, the highest displacement value is 29.79 mm for the transverse direction (Y-axis, and the highest displacement value is 35.32 mm for the longitudinal (X-axis).

3.2 Demand Capacity (D/C) Ratio

This is the result of the bridge D/C ratio obtained from the Csi Bridge software analysis results, which can be seen in Table 2 below.

Table 2: Demand capacity (D/C) ratio result on the bridge

Design Request Name	***Design Category***	***Station* (mm)**	***Direction***	***Demand* (mm)**	***Capacity* (mm)**	**D/C *Ratio***
SEISMIC	D	0	TRANS	11.19	44.77	0.25
SEISMIC	D	0	LONG	11.77	47.10	0.25
SEISMIC	D	65000	TRANS	9.28	37.14	0.25
SEISMIC	D	65000	LONG	4.01	15.46	0.26
SEISMIC	D	75000	TRANS	9.86	39.44	0.25
SEISMIC	D	75000	LONG	3.89	16.58	0.23
SEISMIC	D	195000	TRANS	9.82	39.30	0.25
SEISMIC	D	195000	LONG	3.80	14.19	0.27
SEISMIC	D	205000	TRANS	9.38	37.53	0.25
SEISMIC	D	205000	LONG	3.87	16.01	0.24
SEISMIC	D	270000	TRANS	7.13	28.51	0.25
SEISMIC	D	270000	LONG	2.02	7.76	0.26

Table 2 presents a summary of the demand and capacity values, along with their respective demand-to-capacity (D/C) ratios, for various stations on the bridge under seismic load conditions. The table categorizes the data by design request name (all SEISMIC), design category (D), and the station location along the bridge in mm. The direction of the seismic load is also indicated, either "TRANS" (transverse) or "LONG" (longitudinal). The demand values, representing the structural deformation due to the applied seismic forces, range from 3.89 mm to 11.77 mm across different stations and directions. Capacity, which refers to the structural limit beyond which failure occurs, varies between 15.46 mm and 47.10 mm. The D/C ratio, a critical measure of structural performance, is consistently around 0.25 at most stations, except one station, where the D/C ratio is slightly higher at 0.26. These D/C ratios indicate that the demand is well within the capacity limits for all cases presented, as the D/C values remain below the threshold of 1. This suggests that the bridge, under the considered seismic conditions, retains sufficient strength and stability, maintaining an acceptable safety margin in both longitudinal and transverse directions across the different station locations. Based on the table above, the most significant demand capacity (D/C) ratio value for the steel frame double-track railway bridge is 0.26 for a demand value of 4.01 and a capacity of 15.46. The demand capacity (D/C) ratio value obtained from the seismic analysis results indicates that the bridge belongs to the safe category because the ratio value is less than 1.0.

3. Modal Analysis

Figure 12 illustrates the first mode shape of the truss bridge structure obtained through modal analysis. This deformation pattern predominantly displays vertical translational motion, especially of the deck, which suggests a global flexural mode along the longitudinal axis. This mode reveals symmetric vertical displacements across the span of the bridge.

The deformation is indicative of a vertical bending mode, likely dominated by flexural action in the main truss components. The central span exhibits downward displacement, while the side spans also move in the same phase but with varying magnitudes, implying that the entire bridge deck is vibrating in a coherent manner vertically. This mode is often associated with lower natural frequencies and typically arises from the global flexibility of the structure, particularly in long-span truss bridges with considerable mass and limited vertical stiffness.

Figure 13 illustrates the second mode shape of the truss bridge structure, derived from a finite element modal analysis. This mode is characterized by a complex vertical bending response involving higher-order vibration characteristics across the bridge span. Notably, this deformation pattern reveals two distinct out-of-phase vertical displacements, suggesting the presence of a nodal point near the center of the structure.

In this mode shape, the two side spans exhibit opposing vertical displacements while the central portion shows comparatively minimal motion. Such a mode is representative of a second-order vertical bending mode, where multiple half-wavelengths of vertical deformation appear across the span. This mode reflects a higher natural frequency than the previous one, typically activated by dynamic loads with shorter wavelengths such as high-speed vehicular traffic or localized transient forces.

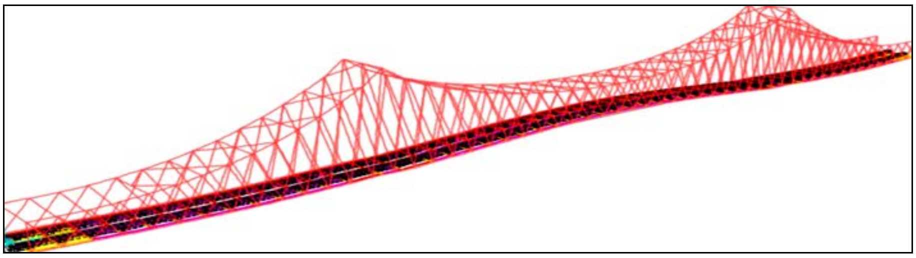

Fig 12: 1st shape mode

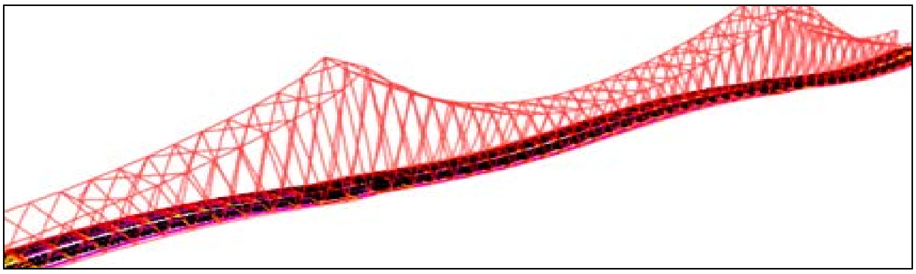

Fig 13: 2nd shape mode

3.4 Load Analysis of Moving Trains

3.4.1 Short Span

Figure 14 presents a plot of bending moment versus station location -span bridge, comparing the structural response under two different loading conditions: one train (blue curve) and two trains (orange curve). The horizontal axis represents the station position along the span, while the vertical axis represents the moment experienced at each station, measured in kN-m. The moments range between positive and negative values, indicating areas of tension and compression, respectively, as the trains traverse the span. The blue curve corresponds to the moment generated by one train passing over the bridge. In the short span condition when only one train crosses the bridge, the maximum moment value is 1.12×10^4 kNm and the minimum moment value is -2.64×10^4 kNm. The curve begins with a positive moment, which decreases as the train moves toward the center of the span, where a significant negative moment is encountered. This negative moment indicates the maximum bending effect at mid-span, caused by the weight of the train. The orange curve represents the moment generated when two trains pass over the bridge simultaneously. In the condition that two trains are crossing the bridge (passing), the maximum moment value is 1.98×10^4 kNm and the minimum value is -3.91×10^4 kNm. Similar to the single-train scenario, the moment starts positive at the beginning of the span, decreases toward the center, and exhibits a more pronounced negative moment at mid-span compared to the single-train case. This indicates that the structural bending is greater when two trains are present, as expected due to the higher loading. Both curves exhibit a V-shaped profile, characteristic of bending moment distributions on simply supported beams. However, the moment values for the two-train scenario are generally higher in magnitude, both positive and negative, indicating the increased demand on the structure when subjected to greater loads. In conclusion, the figure highlights the effect of varying load conditions on the structural behavior of a short-span bridge, demonstrating that the presence of two trains induces significantly higher moments compared to a single train, particularly at the mid-span region, where bending is most critical.

Figure 15 presents a plot comparing the shear force along a short-span bridge at various station locations under two loading scenarios: one train (blue curve) and two trains (orange curve). The horizontal axis represents the station location along the bridge span, ranging from 0 to 15 meters, while the vertical axis represents the shear force. The figure illustrates the variation in shear forces at different points along the span as the train(s) move across the bridge. The blue curve corresponds to the shear force distribution when one train is passing over the span. The maximum value style slide (V2) on only one just passing train bridge is -2.98×10^3 kN and value the minimum is -5.53×10^3 kN. The curve starts with a high positive shear force near the left support of the bridge, gradually decreasing as the station location approaches mid-span. Around the midpoint (between stations 7 and 10), the shear force changes direction and becomes negative, indicating a shift in the force distribution as the train moves toward the opposite end of the span. The orange curve, representing the shear force when two trains are passing, follows a similar pattern but exhibits higher shear forces compared to the one-train case. When two trains cross the bridge (pass each other), the maximum value of the shear force (V2) is 8.53×10^3 kN, whereas marking the minimum is -8.50×10^3 kN. The shear force starts at a higher positive value at the left support and drops more sharply than in the one-train scenario. The negative shear force around mid-span is also more pronounced with two trains, highlighting the increased forces exerted on the bridge when subjected to the heavier load. Both curves display a step-like behavior, which indicates a sudden change in shear force, likely caused by the loading of the train(s) at certain points along the span. This behavior reflects the response of the bridge to concentrated loads moving across it. In summary, the figure illustrates the effect of different loading conditions on shear force distribution along the bridge. The two-train scenario produces higher shear forces, both positive and negative, compared to the one-train scenario, particularly near the supports and mid-span. This information is critical for understanding the structural demand and designing for adequate shear resistance in the bridge.

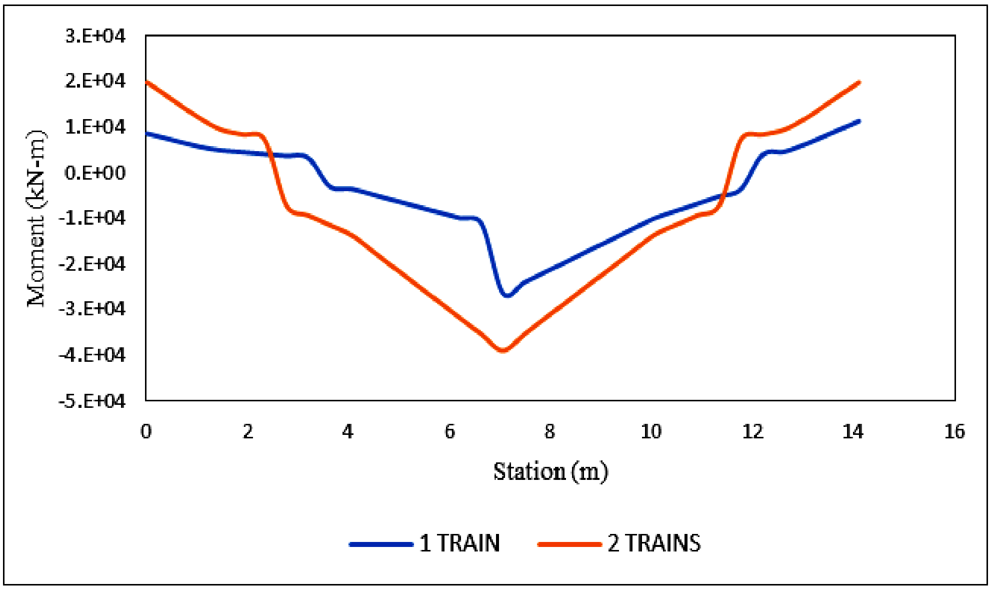

Fig 14: Comparison of moment when one train and two trains pass on a short span

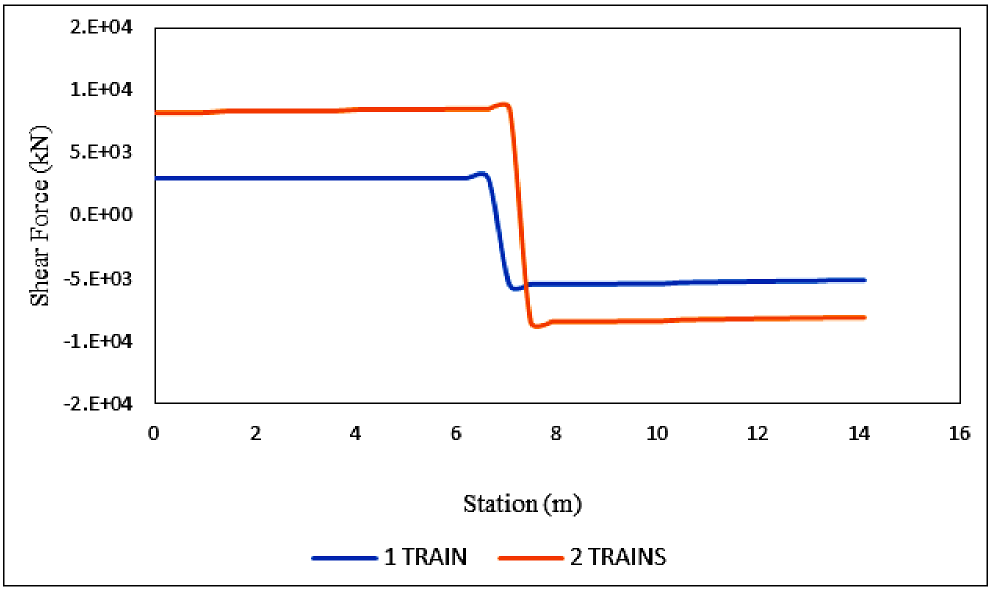

Figure 15. Comparison of shear force when one train and two trains pass on a short span

3.4.2 Long Span

Figure 16 presents a plot of bending moment versus station location along a long-span bridge, comparing the structural response under two different loading conditions: one train (blue curve) The horizontal axis represents the station position along the span, while the vertical axis displays the bending moment. The moments range between positive and negative values, indicating areas of bending tension and compression, respectively, as the trains traverse the span. The blue curve represents the bending moment caused by one train passing over a long span. In the long span condition when only one train crosses the bridge, the maximum moment value is 1.14×10^4 kNm and the minimum value is -2.69×10^4 kNm. The curve begins with a positive moment near the left support, which gradually decreases toward the mid-span, where a significant negative moment occurs. This negative moment is indicative of the maximum bending stress occurring near the center of the span, typical in beam behavior under uniform loading. The orange curve corresponds to the moment generated when two trains pass over the span simultaneously. The maximum moment value in the case of two trains passing or passing through the middle span is 2.00×10^4 kNm, and the minimum moment value is -3.95×10^4 kNm. This curve follows a similar trend, but with slightly lower values in the mid-span region. The negative moment at the center of the span is more pronounced with two trains, reflecting the increased loading from the additional train. Both curves show symmetrical behavior, characteristic of a simply supported span under train loading. Overall, both the one-train and two-train cases exhibit a V-shaped profile, common for bending moment distributions in bridge structures. However, the magnitudes of the moments differ slightly, with the two-train scenario exhibiting larger moments, particularly at the mid-span, due to the increased load. In summary, this figure highlights the effect of loading conditions on the bending moments of a long-span bridge. The comparison between one and two trains passing over the span demonstrates that the structure experiences higher bending moments, particularly in the negative region at mid-span when subjected to the increased load from two trains. Understanding this relationship is crucial for designing the bridge to withstand such forces without failure.

Figure 17 captures how the shear force varies across the span as the trains pass over the bridge. The blue curve corresponds to the shear force distribution when one train crosses the long span. The shear force in the condition of only one train passing through the maximum value is 2.99×10^3 kN, and the minimum value is -5.64×10^3 kN. Initially, there is a high positive shear force near the left support of the bridge, which decreases as the station moves toward mid-span. Around the midpoint of the span, the shear force transitions to negative, indicating a reversal in direction. This behavior is typical of shear force distributions in simply supported spans subjected to moving loads. The orange curve, representing the shear force when two trains pass over the span, follows a similar trend but with higher overall values compared to the one-train case. When two trains are passing or passing each other, the maximum shear force value is 8.64×10^3 kN and the minimum value is -8.60×10^3 kN. Near the left support, the shear force is significantly higher, reflecting the increased load from the second train. The sharp drop in the orange curve at mid-span is more pronounced, with the negative shear force values slightly higher (in magnitude) than those in the one-train scenario, further emphasizing the increased demand on the structure under a heavier load. Both curves display a step-like pattern, which reflects sudden changes in shear force due to the application of the concentrated train loads. The changes are more pronounced with the two-train scenario, which introduces higher forces at critical points along the span. In summary, the figure highlights the impact of varying load conditions (one train vs. two trains) on the shear force distribution along a long-span bridge. The two-train scenario results in larger shear forces, particularly near the supports and mid-span, illustrating the increased structural demand when subjected to heavier loads. This information is critical for ensuring that the bridge is designed with adequate shear resistance to safely accommodate such forces.

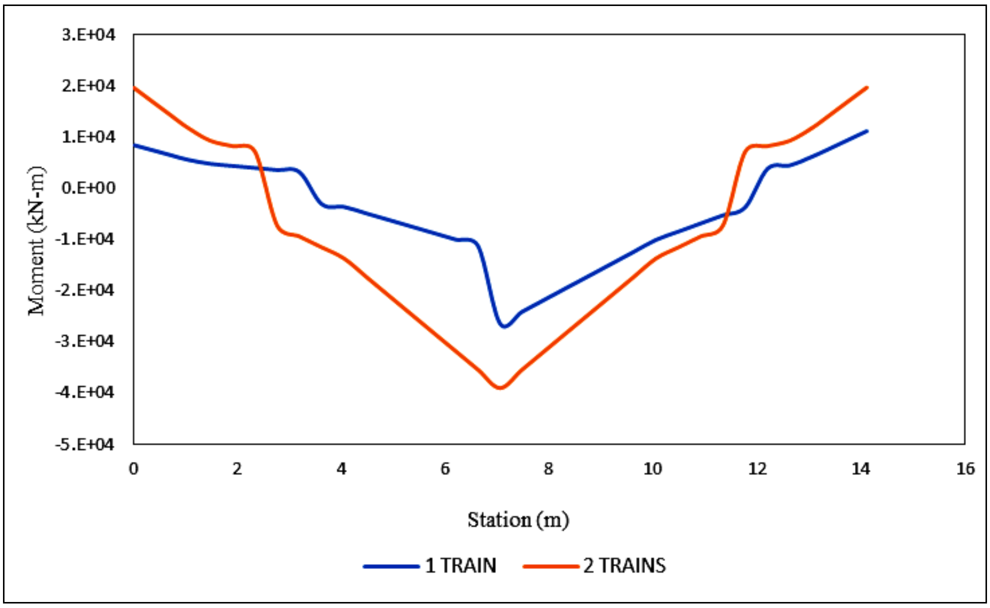

Fig 16: Comparison of moment when one train and two trains pass on a long span

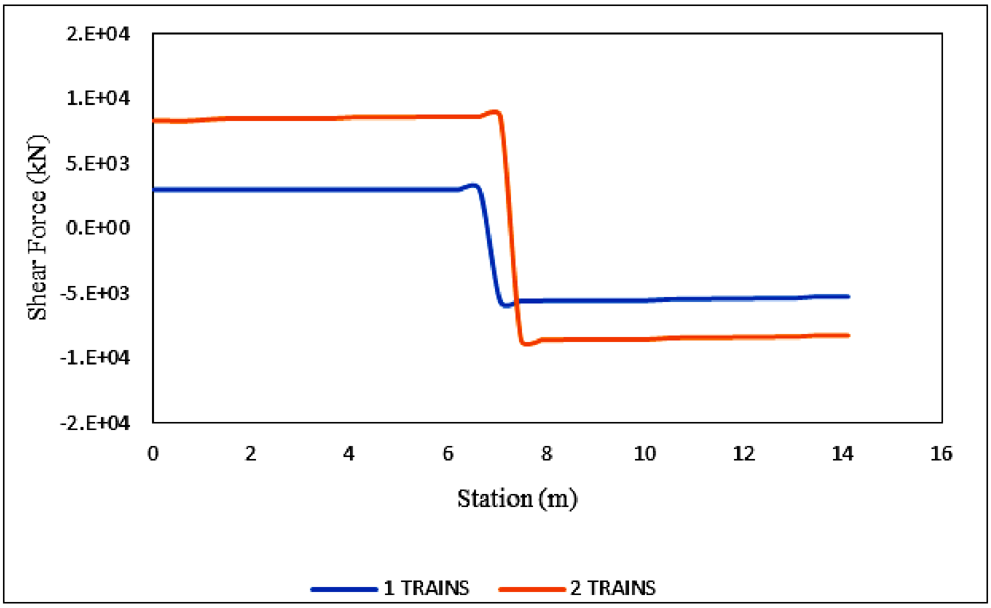

Fig 17: Comparison of shear force when one train and two trains pass on a long span

4. Discussion

The finite element model of the double-track steel railway bridge was successfully developed in CSi Bridge v23 and calibrated to the actual bridge. The model reflects the structural characteristics outlined earlier, emphasizing capacity and stiffness as key factors under seismic and operational loads. Seismic pushover analysis results showed displacement and demand-capacity ratios within safe limits, indicating adequate stiffness and strength to resist seismic forces.

This finding supports the theoretical statement by Kusbiantoro et al. (2023) [11] and Chen et al. (2023) [3], that bridges designed based on proper stiffness considerations are able to maintain structural stability under lateral seismic forces. The results also align with the concept proposed by Riyono et al. (2023) [14], which defines structural capacity as the ability of each component to resist seismic demand. Since the demand-capacity ratio remained below the allowable threshold, the bridge structural elements are considered to still possess adequate resistance.

Furthermore, the modal and vibration behaviors discussed in previous studies, such as Kusumawardani et al. (2024) [9], emphasized that stiffness degradation due to damage can be detected through changes in structural vibration characteristics. The bridge in this study did not exhibit behavioral patterns indicating stiffness reduction, suggesting that no significant deterioration or damage has occurred. Therefore, the bridge is currently functioning within expected structural performance.

The results of the train motion load analysis also confirmed that the structural response increased when two trains passed simultaneously compared to single train loading conditions. This behavior is consistent with the mechanical transmission theory described by Suhary (2000) [17], where dynamic loads are transferred from train wheels to rails, then to bridge components. However, even under multiple train load scenarios, the structural response remained within the safe performance range, indicating that the bridge design adequately anticipates operational loading conditions.

Overall, the findings of this study contribute new insight that the investigated double-track railway bridge is still in a safe and stable condition, both under seismic excitation and operational train load scenarios. This reinforces previous research regarding the importance of accurate finite element modeling and calibration to evaluate real structural performance.

5. Conclusion

The results of the seismic analysis of the bridge with CSi Bridge software using pushover analysis on the 3D finite element model of the steel frame railway double-track bridge obtained displacement values and the ratio of needs and capacity. The highest displacement value is 29.79 mm for the transverse direction (Y axis) located at Pier 3, and the highest displacement value is 35.32 mm for the longitudinal direction (X axis) located at Pier 1. The largest demand capacity (D/C) ratio value is 0.26 for a demand value of 4.01 and a capacity of 15.46, and the smallest demand capacity (D/C) ratio value is 0.23 for a demand value of 3.89 and a capacity of 16.58. The demand capacity (D/C) ratio value obtained from the seismic analysis results using CSi Bridge software indicates that the bridge is classified as a safe category, as the ratio value is less than 1.0.

The results of the analysis of the train motion load on the 3D finite element model of the double-track railway bridge with steel frame type using CSi Bridge software in the form of mark moments and force shifts. From the analysis of the short span condition with only one train passing, the maximum mark moment value is 1.12 × 10^4 kNm. The maximum force shift value is 2.98103 kN, while when two trains are crossing the bridge or passing each other, the maximum mark moment value is 1.98×104 kNm and the maximum force shift value is 8.53×103 kN. The results of the analysis for the long-span condition of one train, which only passes the maximum moment value of 1.14×10^4 kNm and the maximum shear force value of 2.99×10^3 kN, differ when two trains are crossing the bridge. The maximum moment value is 2.00×10^4 kNm, and the maximum shear force value is 8.64×10^3 kN.

References

1. Bencardino F, Curto R, Scavelli V. Inspection and structural rehabilitation of an existing masonry arch railway bridge. Applied Science. 2023;13(5):2973. DOI:10.3390/app13052973.
2. Bagchi A, Raychowdhury P. A comprehensive numerical-based case study on abutment-foundation-backfill behavior of a railway bridge. Transportation Infrastructure Geotechnology. 2023;11(3):1-27. DOI:10.1007/s40515-023-00328-9.
3. Chen CC, Wen HW, Kusbiantoro A, Lai G. Necessity investigation of tie-down devices for single-pylon cable-stayed bridges to resist near-fault earthquakes with finite element models updated by vibration measurements. Structure and Infrastructure Engineering. 2023;19:1-16. DOI:10.1080/15732479.2023.2225053.
4. Chopra A, Goel R. A modal pushover analysis procedure to estimate seismic demands for buildings: theory and preliminary evaluation. Civil and Environmental Engineering. 2001;55:1-28.
5. Guo W, Hu Y, Liu H, Bu D. Seismic performance evaluation of typical piers of China's high-speed railway bridge line using pushover analysis. Mathematical Problems in Engineering. 2019;2019:9514769. DOI:10.1155/2019/9514769.
6. Krawinkler H, Seneviratna GDPK. Pros and cons of a pushover analysis of seismic performance evaluation. Engineering Structures. 1998;20(4-6):452-464. DOI:10.1016/S0141-0296(97)00092-8.
7. Kusumawardani R, Kusbiantoro A, Nugroho U, Upomo TC. Structural health monitoring by identification of dynamic properties and load rating factor at a multi-span prestressed concrete girder bridge. Aceh International Journal of Science and Technology. 2023;12(3):419-432. DOI:10.13170/aijst.12.3.34451.
8. Kusumawardani R, Zelin MA, Kusbiantoro A. Ground vibration analysis of railroad dynamic loads on rail structure. Jurnal Teknik Sipil dan Perencanaan. 2019;21(2):62-70.
9. Kusumawardani R, Kusbiantoro A, Nugroho U, Azizah KP. Structural health monitoring at a single-span prestressed concrete girder bridge by ambient vibration measurement and identification of modal frequency. IOP Conference Series: Earth and Environmental Science. 2024;1381(1):012018. DOI:10.1088/1755-1315/1381/1/012018.
10. Kusbiantoro A, Kusumawardani R, Nugroho U, Hanif N, Azizah KP. Assessment of dynamic properties and finite element model of a single-span concrete girder bridge. International Journal of Engineering. 2025;39(3):13. DOI:10.5829/ije.2026.39.03c.13.
11. Kusbiantoro A, Kusumawardani R, Nugroho U, Hanif N, Azizah KP. Performa penggunaan rubber isolator pada jembatan girder beton. Jurnal Inovasi Konstruksi. 2023;2(1):40-47. DOI:10.56911/jik.v2i1.82.
12. Mosleh A, Hamidi H, Nicknam A, Jara A, Varum H. Seismic vulnerability assessment of concrete railway bridge using nonlinear analyses. Journal of Structural Engineering and Geotechnics. 2016;6(2):41-49.
13. Nuranita B. Evaluasi struktur atas jembatan kereta api WTT dengan modifikasi lebar jalan rel standard gauge. RekaRacana: Jurnal Teknik Sipil. 2023;9(1):46-54. DOI:10.26760/rekaracana.v9i1.46.
14. Riyono CAS, Satyarno I, Setiawan AF, Awaludin A. Pushover analysis in slab-on-piles bridge using reinforced concrete-filled spun piles. IOP Conference Series: Earth and Environmental Science. 2023;1-10.
15. Setiati NR, Surviyanto A. Railway bridge durability test using micrometer analysis. Civil Engineering Dynamics: Civil Engineering Scientific Magazine. 2013;13(2):54-59.
16. Shatarat N, Shehadeh M, Naser M. Impact of plastic hinge properties on capacity curve of reinforced concrete bridges. Advances in Materials Science and Engineering. 2017;2017:6310321. DOI:10.1155/2017/6310321.
17. Suhairy SAL. Prediction of ground vibration from railways. Borås: SP Swedish National Testing and Research Institute; 2000.
18. Vičan J, Gocál J, Odrobiňák J, Koteš P. Existing steel railway bridges evaluation. Civil and Environmental Engineering. 2016;12(2):103-110. DOI:10.1515/cee-2016-0014.
19. Wu WH, Chen CC, Kusbiantoro A, Lai G. Finite element model of a cable-stayed bridge updated with vibration measurements and its application to

investigate the variation of modal frequencies in monitoring. Structure and Infrastructure Engineering. 2022;18:1-11. DOI:10.1080/15732479.2022.2132517.

20. Yamato T, Umehara T, Aoki H, Nakamura S, Ezaki J, Suetomi K. Damage to Daikai subway station of Kobe rapid transit system and estimation of its cause during the 1995 Hyogoken-Nanbu earthquake. Doboku Gakkai Ronbunshu. 1996;537:303-320. DOI:10.2208/jscej.1996.537_303.
21. Yang Y, Cao J, Qu R, Xu Z. Numerical simulation of the seismic damage of Daikai station based on pushover analyses. Buildings. 2023;13(3):760. DOI:10.3390/buildings13030760.
22. Zhang Y, Chen X, Zhang X, Ding M, Wang Y, Liu Z. Nonlinear response of the pile group foundation for lateral loads using pushover analysis. Earthquakes and Structures. 2020;19(4):273-286. DOI:10.12989/eas.2020.19.4.273.